Molecular Mechanism of the Sea Anemone Toxin ShK Recognizing the Kv1.3 Channel Explored by Docking and Molecular Dynamic Simulations

Ling Jin*,† and Yingliang Wu*,‡

Department of Applied Chemistry, School of Natural Science, Wuhan University of Technology, Wuhan, Hubei 430070, P.R. China, and State Key Laboratory of Virology, College of Life Sciences, Wuhan University, Wuhan, Hubei 430072, P.R. China

Received May 26, 2007

Computational methods are employed to simulate the interaction of the sea anemone toxin ShK in complex with the voltage-gated potassium channel Kv1.3 from mice. All of the available 20 structures of ShK in the Protein Data Bank were considered for improving the performance of the rigid protein docking of ZDOCK. The traditional and novel binding modes were obtained among a large number of predicted complexes by using clustering analysis, screening with expert knowledge, energy minimization, and molecular dynamic simulations. The quality and validity of the resulting complexes were further evaluated to identify a favorable complex structure by 500 ps molecular dynamic simulations and the change of binding free energies with a computational alanine scanning technique. The novel and reasonable ShK-Kv1.3 complex structure was found to be different from the traditional model by using the Lys22 residue to block the channel pore. From the resulting structure of the ShK-Kv1.3 complex, ShK mainly associates the channel outer vestibule with its second helical segment. Structural analysis first revealed that the Lys22 residue side chain of the ShK peptide just hangs between C and D chains of the Kv1.3 channel instead of physically blocking the channel pore. The obvious loss of the ShK Ser20Ala and Tyr23Ala mutant binding ability to the Kv1.3 channel is caused by the conformational change. The five hydrogen bonds between Arg24 in ShK and H404(A) and D402(D) in Kv1.3 make Arg24 the most crucial for its binding to the Kv1.3 channel. Besides the detailed interaction between ShK and Kv1.3 at the atom level, the significant conformational change induced by the interaction between the ShK peptide and the Kv1.3 channel, accompanied by the gradual decrease of binding free energies, strongly implies that the binding of the ShK peptide toward the Kv1.3 channel is a dynamic process of conformational rearrangement and energy stabilization. All of these can accelerate the development of ShK structure-based immunosuppressants.

INTRODUCTION

Potassium channels are a diverse and ubiquitous family of membrane proteins in both excitable and nonexcitable cells. The voltage-gated Kv1.3 channel in human T lymphocytes plays an important role in calcium signaling, activation, adhesion, and migration and has therefore been regarded as a considerably attractive target for immunotherapy through selective blockage.[1−3] Numerous peptides isolated from scorpion venoms and sea anemone can potently recognize Kv1.3 channels. For example, ShK, a 35-residue polypeptide toxin from the sea anemone, *Stichodactyla helianthus*, is able to block Kv1.3 ($K_d \sim 10$ pM), suppress proliferation of effector memory T cells at picomolar concentrations,[2] and ameliorate experimental autoimmune encephalomyelitis.[1] Due to its excellent pharmacological activity, now ShK and its analogs are currently undergoing further evaluation as leads in the development of new biopharmaceuticals for the treatment of multiple sclerosis and other T-cell mediated autoimmune disorders.[4,5]

Similar to well-known scorpion toxin ChTX, ShK has a well defined conformation constrained by three disulfide bonds (Figure 1A,B) However, the pairing pattern of disulfide linkages for ShK significantly differs from that of ChTX, and, besides, ShK lacks a stable β-sheet secondary structure, while ChTX and most other scorpion toxins have β-sheet domains at both ends of the molecule. Different structures determine different types of their epitopes. ShK mainly uses a helical domain, composed of the Ser20-Arg24 fragment, to recognize the Kv1.3 channel vestibule,[6] and ChTX mainly uses β-sheet domains to associate potassium channels.[7,8] In the modeled potassium channel-ChTX complex structure, the most critical residue Lys27 physically blocks the channel pore, and other spatially adjacent Arg25, Asn30, Arg34, and Tyr36 residues from the β-sheet domain are very important to toxin binding afiinity.[8] Therefore, a reasonable Kv1.3-ShK complex structure is greatly needed not only for understanding the diverse interactions between potassium channels and inhibitory peptides but also for rational design of specific ShK analogs with the potential to be used clinically as immunosuppressants.

Protein−protein docking techniques for predicting protein−protein complex structures are recently making a great deal of progress in the community-wide experiment on Critical Assessment of PRedicted Interactions (CAPRI).[9−11] The

* Corresponding author e-mail: jling2002@163.com (L.J.) and phone: ++86-(0)-27-68752831; fax: ++86-(0)-27-68752146; e-mail: ylwu@whu.edu.cn (Y.W.).

† Wuhan University of Technology.

‡ Wuhan University.

10.1021/ci700178w CCC: $37.00
Published on Web 08/25/2007

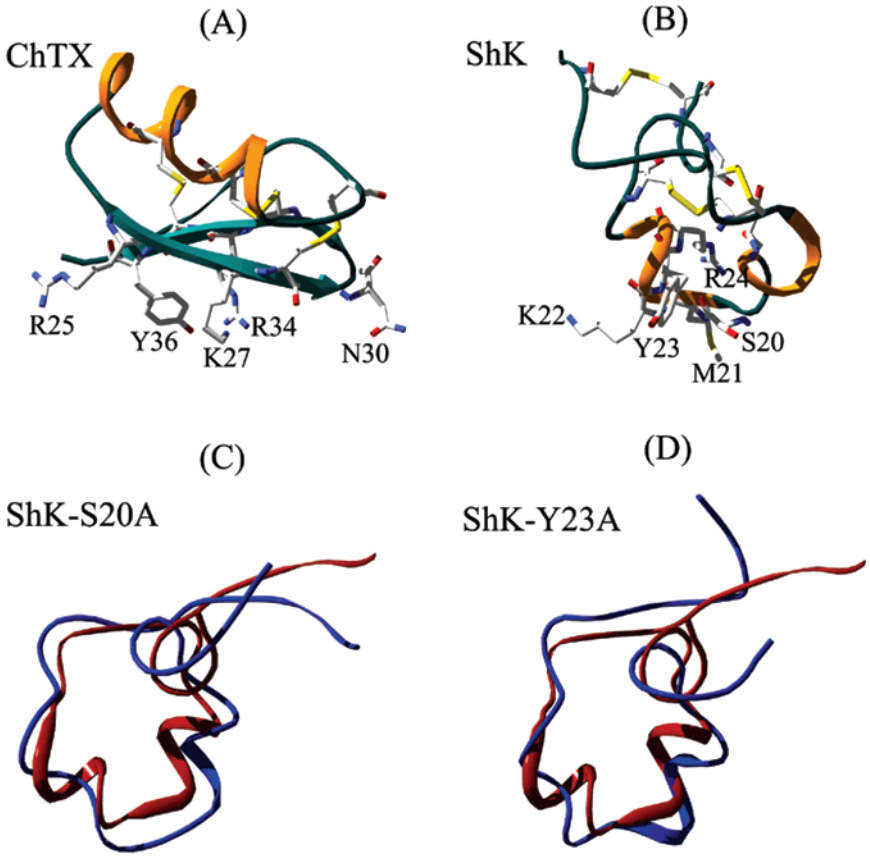

Figure 1. Structures of scorpion toxin ChTX and sea anemone toxin ShK with differential disulfide bridges. Parts A and B: three disulfide bridges are organized by the C1−C4, C2−C5, and C3−C6 in ChTX and by the C1−C6, C2−C4, and C3−C5 in ShK, respectively. The main functional residues are labeled in their structures, respectively. Parts C and D are ShK-S20A and ShK-Y23A mutant structure (6 ns MD simulations) differences from the ShK structure, respectively. The red and blue structures stand for wild-type and mutant conformations, respectively.

ZDOCK procedure, developed by the Weng group,[12−14] achieved a good performance during the CAPRI challenge and was used to successfully simulate scorpion toxin ScyTx interaction with a small conduction calcium-activated potassium channel combined with molecular dynamic simulations.[15] In this work, we attempt to model ShK in a complex with the Kv1.3 channel from a mouse and reveal its molecular mechanism of recognizing the Kv1.3 channel for accelerating the development of ShK structure-based immunosuppressants.

METHODS AND THEORY

Atomic Coordinates. The atomic coordinates of ShK (PDB code: 1ROO) were downloaded from the Protein Data Bank.[16] The potassium channel from *Streptomyces lividans* (KcsA) is an integral membrane protein with sequence similarity to most potassium channels, particularly in the pore region seen from the sequence alignment of the selected K^+ channel with various types[17] and demonstrated by the mammalian Kv1.2 structure.[18] The homologous spatial structure of the pore region of Kv1.3 was modeled by using the close-state structure of the KcsA channel (PDB code: 1BL8) as a template through the SWISS-MODEL server.[19] The modeled structure of Kv1.3 was subjected to refinement by a 500-step energy minimization by the SANDER module in the AMBER 8 suite of programs.[20]

Protein−Protein Docking. All 20 ShK conformations from NMR were used for improving the rigid docking performance of the molecular docking algorithm ZDOCK (generously provided by Dr. Zhiping Weng from the Boston University), which is a Fast Fourier Transform (FFT)-based, initial-stage rigid-body docking algorithm.[12−15] The good accuracy of ZDOCK on predicting protein complexes has been proved by its good performances in the CAPRI Challenge.[10,14] Clustering and the application of biological information along with ZDOCK, followed by a 500-step energy minimization for each possible toxin-channel complex using the SANDER module in the AMBER 8 suite of programs as well as calculating the ligand−receptor interaction energies with the ANAL program of AMBER 8, were employed for identifying appropriate candidate complexes for further MD simulations from docking results.

In this work, the membrane around the channel has not been considered during the simulation because many simulation studies on the recognition between scorpion toxins and potassium channels without a membrane included have achieved good agreements with experimental data.[15, 21, 22] In addition, this membrane-ignored treatment can facilitate the computations greatly.

Molecular Dynamic Simulations. Further a 10 ps MD simulation was carried out using the distance-dependent dielectric with a time step of 2.0 fs. The nonbonded cutoff was set to 12.0 Å, and heavy atoms were restrained with a force constant of 5.0 kcal/mol/Å.[2] The most plausible binding mode of the ShK-Kv1.3 complex was screened by interactive energy calculated by the ANAL program and structural

analysis based on the structural-functional experiments.[6]

In the comparison of binding free energies of different ShK orientations in complex with Kv1.3, it is important to ensure that each of these systems is sufficiently equilibrated ahead of data collection and analysis. In our work, the Generalized Born (GB)[23] solvation model in macromolecular simulations was used instead of explicit water during more sufficient MD simulation. GB-MD simulations (500 ps) (igb=2) were carried out at 300 K with a time step of 2.0 fs. A cutoff distance of 12 Å was used for the nonbonded interaction. We repeated the equilibration step several times starting from a larger force constant of 5.0 kcal/mol/ Å^2 and then gradually reducing it to zero so that more conformational flexibility was introduced. In addition, the channel S5 and S6 segments were restrained by a force constant of 1.0 kcal/mol/Å^2 during MD simulation, as these segments are buried in the membrane and have no effect on the recognition of ShK. Such a hypothesis is based on the result that no conformational change in the S5 and S6 helixes was observed by solid-state NMR for the K^+ channel.[31] The ff99 force field (Parm99)[24] was used throughout the energy minimization and MD simulations, which were carried out by using the Amber 8 program on a 32-CPU Dawning TC4000L cluster (Beijing, China). The detailed procedures of molecular dynamic simulations were described previously.[25]

Calculation of Binding Free Energy by MM-PBSA. In the MM-PBSA of AMBER 8.0, the binding free energy of A+B → AB is calculated using the following thermodynamic cycle

$$\begin{array}{ccccc} A_{aqu} & + & B_{aqu} & \xrightarrow{\Delta G_{binding}} & AB_{aqu} \\ \downarrow -\Delta G^{A}_{solv} & & \downarrow -\Delta G^{B}_{solv} & & \downarrow -\Delta G^{AB}_{solv} \\ A_{gas} & + & B_{gas} & \xrightarrow{\Delta G_{gas}} & AB_{gas} \end{array}$$

$$\begin{aligned} \Delta G_{binding} &= \Delta G_{gas} - \Delta G^{A}_{solv} - \Delta G^{B}_{solv} + \Delta G^{AB}_{solv} \\ &= \Delta H_{gas} - T\Delta S - \Delta G^{A}_{GBSA} - \Delta G^{B}_{GBSA} + \Delta G^{AB}_{GBSA} \\ &= \Delta H_{gas} - T\Delta S - \Delta\Delta G_{GB} + \Delta\Delta G_{SA} \end{aligned} \quad (1)$$

$$\Delta H_{gas} \approx \Delta E_{gas} = \Delta E_{intra} + \Delta E_{elec} + \Delta E_{vdw} \quad (2)$$

$$\Delta\Delta G_{GB} = \Delta G^{AB}_{GB} - (\Delta G^{A}_{GB} + \Delta G^{B}_{GB}) \quad (3)$$

$$\Delta\Delta G_{SA} = \Delta G^{AB}_{SA} - (\Delta G^{A}_{SA} + \Delta G^{B}_{SA}) \quad (4)$$

where T is the temperature, S is the solute entropy, ΔG_{gas} is the interaction energy between A and B in the gas phase, and ΔG^{A}_{solv}, ΔG^{B}_{solv}, and ΔG^{AB}_{solv} are the solvation free energies of A, B, and AB, which are estimated using a GB surface area (GBSA) method,[32,33,37] i.e., $\Delta G^{AB}_{solv} + \Delta G^{AB}_{GBSA} + \Delta G^{AB}_{GB} + \Delta G^{AB}_{SA}$, etc. ΔG_{GB} and ΔG_{SA} are the electrostatic and nonpolar terms, respectively. ΔE_{bond}, ΔE_{angle}, and $\Delta E_{torsion}$ are contributions to the intramolecular energy ΔE_{intra} of the complex. E_{vdW} is the van der Waals (vdW) interaction energy. Because of the constant contribution of $-T\Delta S$ for each docked complex, we quote $\Delta G^*_{binding}$, which is $\Delta G_{binding} + T\Delta S$ in the discussion. For the purpose of verifying the quality and validity of every resulting Kv1.3-ShK complex obtained, the relative binding free energy $\Delta G^*_{binding}$ was calculated by using MM-PBSA for postprocessing collected snapshots from the MD trajectories.

RESULTS AND DISCUSSION

The Main Binding Modes Screened by ZDOCK and MD Simulations. The alanine-scanning experiments were carried out for characterizing the interaction between the ShK peptide and the Kv1.3 channel, and the residual segment Ser20-Arg24 is essential to the binding affinity of the ShK peptide,[6] which is helpful to improve the ZDOCK performance. During the ZDOCK prediction, both the ShK peptide and the Kv1.3 channel were treated as rigid bodies, thus the effect of residue flexibility was neglected. To further improve the docking performance, each available NMR conformation of ShK was considered. After energy minimization of the ZDOCK structures and further 10 ps MD simulations using the distance-dependent dielectric combined with experimental data, two main binding modes were obtained (Figure 2A,A′). It can be seen that the second helical segment, encompassing critical residues 22−24 of the ShK peptide, is mainly used to recognize the Kv1.3 channel vestibule, which is inconsistent with the experimental data.[6] However, there is an obvious difference between the two binding modes. In binding mode I, the side chain of Lys22, similar to widely recognized Lys27 in ChTX,[8] plugs into the Kv1.3 channel pore.[6,26,27] In contrast, the side chain of Lys22 hangs between C and D chains in the novel binding mode II, which is also not seen in the binding modes of known scorpion toxins ChTX, AgTX2, and ScyTx.[8,15,21]

Before further identifying a more reasonable binding mode, the backbone and side-chain flexibility of complex structures was introduced by 500 ps MD simulations. The corresponding restraint was gradually reduced from protein backbone and side-chain atoms to only backbone atoms during the initial 210 ps MD simulations. As shown in Figure 3, the root mean-square deviation (RMSD) values of backbone and all heavy atoms compared with the starting complex vary little during the last 150 ps MD simulations, which indicated that the system was equilibrated for a complex structure in binding mode II. The similar RMSD trajectory was also obtained for the Kv1.3-ShK structure in binding mode I (data not shown). Based on the two equilibrated complex structures, their further discrimination was carried out in the following.

Discrimination of Binding Modes Assisted by Computational Alanine Scanning. The computational alanine scanning technique[28] was widely used to calculate the difference in the binding free energies between mutated and wild-type complexes for identifying a reasonable channel-peptide complex structure.[15,21] In this work, this technique was also used to discriminate between two binding modes of Kv1.3-ShK complexes. As shown in Figure 4B, an overall good agreement was found between the calculated and experimental data profiles for the Kv1.3-ShK complex in the novel binding mode II. Among three critical Lys22, Tyr23, and Arg24 residues of ShK, the calculated data of binding free energy change for Lys22 and Arg24 residues are in very good agreement with the experimental results,[6] and there are no inconsistencies for the ShK-Y23A mutant

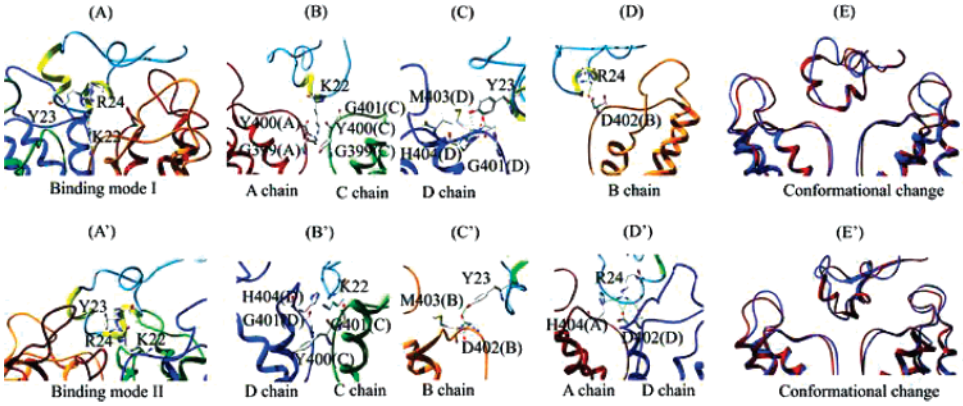

Figure 2. The possible ShK-Kv1.3 structures and their recognition mechanism. Parts A and E and A′ and E′ represent the ShK-Kv1.3 structure and the recognition mechanism for binding modes I and II, respectively. Parts B−D and B′−D′ represent the plausible interaction between function residues of the ShK peptide and residues of the Kv1.3 channel within a contact distance of 4.0 Å. In parts E and E′, the red and blue complex structures stand for unbound and bound conformations, respectively. The dotted line represents the hydrogen bond between two atoms.

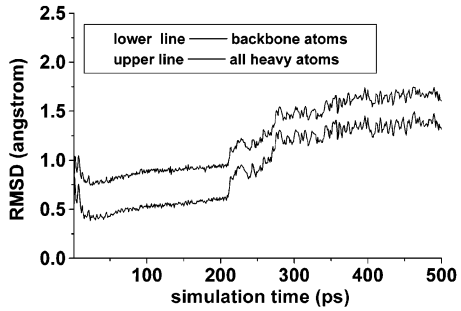

Figure 3. Root-mean-square deviations (Å) of all heavy atoms (upper line) and the backbone atoms (lower line) of the ShK-Kv1.3 complex during 500 ps MD simulations compared with the docked structure.

due to the conformational change. The RMSD of Cα atoms rises to 3.10 Å between wild-type ShK and equilibrated Shk-Y23A mutant structures (6 ns MD simulations) (Figure 1D). Such a conformational change affecting binding peptide affinity is also found for ShK-S20A (Figure 1C) and ShK-L25A mutants (figure not shown). On the contrary to the Ser20 residue, there is little difference between the calculated and experimental results for an important Met21 residue. In addition, the calculated data also agree well with the experimental data for other unimportant and partially moderately important residues of the ShK peptide (Figure 4B).

Different from binding mode II, there is no good relativity for most residues between the calculated and experimental data profile in binding mode I (Figures 2A and 4A). There is the biggest change of calculated binding free energy for Lys22, which is surrounded by the residues from the channel selectivity filter (Figure 2B), and such a value is much higher than the experimental data. For other two crucial Tyr23 and Arg24 residues, there are much bigger differences between calculated and experimental data although hydrogen bonds are formed between residues from ShK and Kv1.3 (Figure 2C,D). In addition, the calculated data for Lys9 and Arg29 residues are far from the experimental results (Figure 4A). The profile comparison of computational alanine scanning data with experimental alanine scanning data strongly suggests that the Kv1.3-ShK complex structure in binding mode II is reasonable.

Recognition Mechanism between the Kv1.3 Channel and the ShK Peptide. The favorable Kv1.3-ShK complex

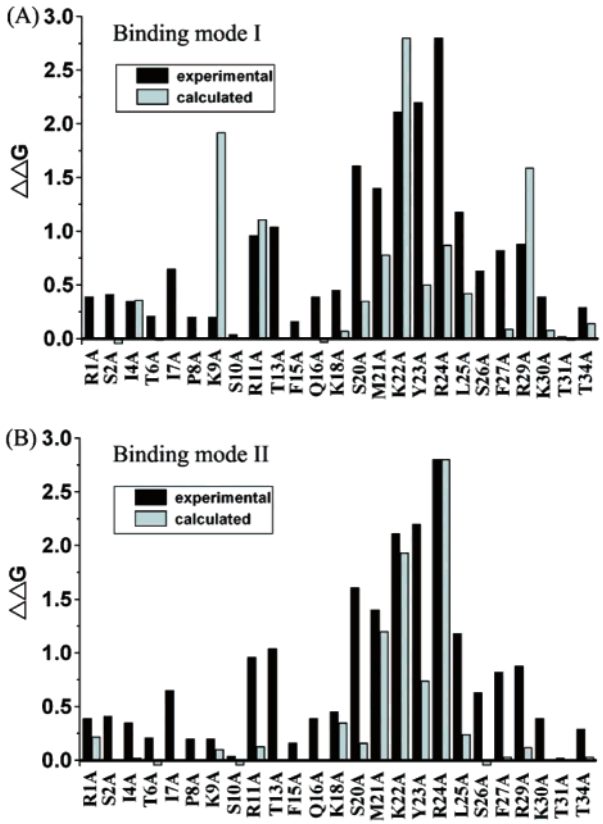

Figure 4. Comparison of calculated and experimental effects for ShK mutations on the binding affinity. Parts A and B are the comparisons of calculated and experimental data for binding modes I and II, respectively. Calculated data are normalized, whereas experimental data are from previous experiments.[6]

structure reveals novel recognition mechanism between the Kv1.3 channel and the ShK peptide. The most significant difference is that there is no channel pore-blocking residue in the ShK peptide, which is different from well-known scorpion toxins ChTX, AgTX2, OSK1 analogs, and ScyTx.[8,15,21,29,30] The side chain of Lys22 was ever thought to block the Kv1.3 channel pore in binding mode I,[6,26,27] and now it hangs between C and D chains of the Kv1.3 channel and is surrounded by Tyr400(C), Gly401(C), Gly401(D), and H404(D) within a contact distance of 4.0 Å (Figure 2B′). The essential Tyr23 can interact with Asp402(B) and

Table 1. Dynamic Change of Relative Binding Free Energies from Representative ShK-Kv1.3 Conformations during the Binding Process

complex	ΔE_{elec}	ΔE_{vdW}	ΔE_{inter}	$\Delta\Delta G_{GB}$	$\Delta\Delta G_{SA}$	$\Delta G_{binding}$[a]
initial conformation	−1854.48	−66.68	−1921.16	1916.93	−8.49	−12.72
intermediate conformation[b]	−1870.18	−67.46	−1973.64	1919.08	−8.63	−27.19
final conformation	−2072.33	−81.85	−2154.18	2120.47	−10.92	−44.63

[a] All energies are in kcal/mol. [b] Intermediate conformation refers to the ShK-Kv1.3 complex structure extracted at the end of 210 ps MD simulations.

Met403(B) near the channel selectivity filter in company with an hydrogen bond (Figure 2C′). The obvious decrease of the binding ability is caused by the conformational change when the Tyr23 was replaced by Ala23 in ShK (Figure 1D), because a similar change is found for the Tyr23 residue in binding mode I (Figure 2C). More interesting, there are five unexpected hydrogen bonds between Arg24 of ShK and H404(A) and D402(D), which demonstrates that the Arg24 residue is the most crucial for its binding to the Kv1.3 channel (Figure 2D′).[6] For the important Met21 residue, it is similar to Lys22 with its side chain hanging between A and D chains of Kv1.3 channels. The side chain of Met21 is surrounded by G401(A), Met403(A), H404(A), Tyr400(D), and Asp402(D) within a contact distance of 4.0 Å (figure not shown). As for other unimportant residues in the ShK peptide, they are far from the kv1.3 channel vestibule so that there is a slight effect on ShK binding activities.

A derivative of ShK, referred to as the ShK-Dap22 peptide with a shorter side chain (PDB code: 1BEI), was ever found to be more selective for Kv1.3 than native ShK.[31] Subsequently, the ShK-Dap[22] peptide was proposed to have the binding mode toward the Kv1.3 channel, which is similar to binding mode II in our work. There is only a three methylene difference for the side chain between the Lys22 residue in ShK and Dap22 in the ShK analog; therefore, their overall binding modes are likely similar. Here, both Dap22 and Lys22 are in the vicinity of the His404 residue in the Kv1.3 channel,[32] which was later demonstrated to be critical for the peptide affinity among Kv1.x channels.[33,34]

In summary, the recognition mechanism of the ShK peptide binding to the Kv1.3 channel was revealed according to the obtained favorable Kv1.3-ShK complex structure, which is different from the traditionally proposed structure model. Recently, another AOSK1 peptide was also characterized to be the most potent Kv1.3 blocker,[29,30] and it would be significantly informative to compare the AOSK1-Kv1.3 and ShK-Kv1.3 complex structures in the near future. In addition, our obtained structure can further enrich the functional dyad of natural toxins.[35]

Conformational Change Induced by the Recognition. More lately, Lange et al. proposed that the structural flexibility of the K^+ channel and the toxin represented an important determinant for the highly specific toxin-K^+ channel recognition, and especially conformational flexibility in the interface between the potassium channel and the inhibitory peptide was found by the solid-state NMR.[36] Such conformational flexibility, induced by the interaction of ShK with the Kv1.3 channel, was also observed for two main binding modes in this work (Figure 3). During the initial 210 ps MD simulations, the RMSDs of the backbone and all the heavy atoms slightly increase with a gradually decreased force constant from both the backbone and the side-chain atoms to only backbone atoms. Then the more significant RMSD value change was found in the subsequent 290 ps MD simulations after the restraint was removed. Through comparing the final and starting ShK-Kv1.3 complexes, significant structural rearrangements were detected in both ShK and the Kv1.3 channel (Figure 2E′). The RMSD values of backbone and side-chain atoms rose to 2.09 Å and 4.09 Å for bound and unbound ShK structures, respectively. Simultaneously, there is an emergence of two β-sheet segments encompassing residues 4−6 and 27−29 (Figure 2E′), which is induced by the interaction with the Kv1.3 channel. Besides a conformational change in the ShK peptide, considerable structural changes were seen in the channel outer vestibule, which forms the channel interface (Figure 2E′). The RMSD values of backbone and side-chain atoms are 1.50 Å and 2.18 Å between the bound and the unbound Kv1.3 channel, respectively. Especially large conformational changes were found in the selectivity filter and channel turrets, which were affected by the ShK binding.

During the interacting of ShK and the Kv1.3 channel, the conformational arrangement indicated that the contacts between ShK and Kv1.3 were strengthened gradually, and calculations of binding free energies of complexes in the binding process greatly supported this finding. A very harmonious stepwise process of energy minimizing was found to be associated with the forming of a stable complex (Table 1), which demonstrated that the ShK recognition was the reduction of binding free energy in conjunction with a tighter interaction toward the target channel.

In conclusion, the change of both conformation and interactive energy not only provides the basis for formation of a tight complex with the active sites of the K^+ channel but also may be a crucial prerequisite for the high-affinity ligand binding to an ion channel.

CONCLUSION

The most optimized structure of the ShK peptide in a complex with the Kv1.3 channel was determined by ZDOCK with MD simulations followed by computational alanine scanning analysis. The final refined structure of ShK and the Kv1.3 channel agrees well with the experimental alanine scanning data. The Lys22 residue side chain of the ShK peptide just hangs between C and D chains of the Kv1.3 channel instead of physically blocking the channel pore. The obvious loss of binding ability to the Kv1.3 channel is caused by the conformational change of the ShK Tyr23Ala mutant. The five hydrogen bonds between Arg24 in ShK and H404-(A) and D402(D) in Kv1.3 make the Arg24 the most crucial for its binding to the Kv1.3 channel. Besides the detailed interaction between ShK and Kv1.3 at the atom level, the significant conformational change induced by the interaction between the ShK peptide and the Kv1.3 channel, accompanied by the gradual decrease of binding free energies, strongly implies that the binding of the ShK peptide toward the Kv1.3 channel is a dynamic process of conformational

rearrangement and energy stabilization. The reasonable ShK-Kv1.3 complex structure not only efficiently reveals the specificity mechanism of ShK recognizing the target Kv1.3 channel but also accelerates the development of ShK structure-based immunosuppressants. Simultaneously, the rigid ZDOCK combined with MD simulations followed by computational alanine scanning analysis is an attractive approach for modeling inhibitory peptide-potassium channel complexes a priori for further biological studies.

REFERENCES AND NOTES

(1) Beeton, C.; Wulff, H.; Barbaria, J.; Clot-Faybesse, O.; Pennington, M.; Bernard, D.; Cahalan, M.; Chandy, K.; Beraud, E. Selective blockade of T lymphocyte K^+ channels ameliorates experimental autoimmune encephalomyelitis, a model for multiple sclerosis. *Proc. Natl. Acad. Sci. U.S.A.* **2001**, *98*, 13942−13947.

(2) Wulff, H.; Calabresi, P.; Allie, R.; Yun, S.; Pennington, M. W.; Beeton, C.; Chandy, K. G. The voltage-gated Kv1.3 K+ channel in effector memory T cells as new target for MS. *J. Clin. Invest.* **2003**, *111*, 1703−1713.

(3) Chandy, K. G.; Wulff, H.; Beeton, C.; Pennington, M.; Gutman, G. A.; Cahalan, M. D. K^+ channels as targets for specific immunomodulation. *Trends Pharmacol. Sci.* **2004**, *25*, 280−289.

(4) Beeton, C.; Pennington, M. W.; Wulff, H.; Singh, S.; Nugent, D.; Crossley, G.; Khaytin, I.; Calabresi, P. A.; Chen, C. Y.; Gutman, G. A.; Chandy, K. G. Targeting effector memory T cells with a selective peptide inhibitor of Kv1.3 channels for therapy of autoimmune diseases. *Mol. Pharmacol*. **2005**, *67*, 1369−1381.

(5) Beeton, C.; Wulff, H.; Standifer, N. E.; Azam, P.; Mullen, K. M.; Pennington, M. W.; Kolski-Andreaco, A.; Wei, E.; Grino, A.; Counts, D. R.; Wang, P. H.; LeeHealey, C. J.; Andrews, B. S.; Sankaranarayanan, A.; Homerick, D.; Roeck, W. W.; Tehranzadeh, J.; Stanhope, K. L.; Zimin, P.; Havel, P. J.; Griffey, S.; Knaus, H. G.; Nepom, G. T.; Gutman, G. A.; Calabresi, P. A.; Chandy, K. G. Kv1.3 channels are a therapeutic target for T cell-mediated autoimmune diseases. *Proc. Natl. Acad. Sci. U.S.A.* **2006**, *103*, 17414−17419.

(6) Rauer, H.; Pennington, M.; Cahalan, M.; Chandy, K. G. Structural conservation of the pores of calcium-activated and voltage-gated potassium channels determined by a sea anemone toxin. *J. Biol. Chem*. **1999**, *274*, 21885−21892.

(7) Goldstein, S. A.; Pheasant, D. J.; Miller, C. The charybdotoxin receptor of a Shaker K^+ channel: peptide and channel residues mediating molecular recognition. *Neuron* **1994**, *12*, 1377−1388.

(8) Yu, L.; Sun, C.; Song, D.; Shen, J.; Xu, N.; Gunasekera, A.; Hajduk, P. J.; Olejniczak, E. T. Nuclear Magnetic Resonance Structural Studies of a Potassium Channel-Charybdotoxin Complex. *Biochemistry* **2005**, *44*, 15834−15841.

(9) Gray, J. J.; Moughon, S. E.; Kortemme, T.; Schueler-Furman, O.; Misura, K. M. S.; Morozov, A. V.; Baker, D. Protein−protein docking predictions for the CAPRI experiment. *Proteins* **2003**, *52*, 118−122.

(10) Mendez, R.; Leplae, R.; Lensink, M. F.; Wodak, S. J. Assessment of CAPRI predictions in rounds 3−5 shows progress in docking procedures. *Proteins* **2005**, *60*, 150−169.

(11) Smith, G. R.; Fitzjohn, P. W.; Page, C. S.; Bates, P. A. Incorporation of flexibility into rigid-body docking: applications in rounds 3−5 of CAPRI. *Proteins* **2005**, *60*, 263−268.

(12) Chen, R.; Li, L.; Weng, Z. P. ZDOCK: An initial-stage protein-docking algorithm. *Proteins* **2003**, *52*, 80−87.

(13) Chen, R.; Tong, W. W.; Mintseris, J.; Li, L.; Weng, Z. P. ZDOCK predictions for the CAPRI challenge. *Proteins* **2003**, *52*: 68−73.

(14) Wiehe, K.; Pierce, B.; Mintseris, J; Tong, W. W.; Anderson, R.; Chen, R.; Weng, Z. P. ZDOCK and RDOCK performance in CAPRI rounds. *Proteins* **2005**, *60*, 207−213.

(15) Wu, Y. L.; Cao, Z. J.; Yi, H.; Jiang, D. H.; Mao, X.; Liu, H.; Li, W. X. Simulation of the interaction between ScyTx and small conductance calcium-activated potassium channel by docking and MM-PBSA. *Biophys. J.* **2004**, *87*, 105−112.

(16) Berman, H. M.; Westbrook, J.; Feng, Z.; Gilliland, G.; Bhat, T. N.; Weissig, H.; Shindyalov, I. N.; Bourne, P. E. The protein data bank. *Nucleic Acids Res.* **2000**, *28*, 235−242.

(17) Doyle, D. A.; Cabral, J. M.; Pfuetzner, R. A.; Kuo, A.; Gulbis, J. M.; Cohen, S. L.; Chait, B. T.; MacKinnon, R. The structure of the potassium channel: molecular basis of K^+ conduction and selectivity. *Science* **1998**, *280*, 69−77.

(18) Long, S. B.; Campbell, E. B.; MacKinnon, R. Crystal structure of a mammalian oltage-dependent Shaker family K^+ Channel. *Science* **2005**, *309*, 897−903.

(19) Guex, N.; Peitsch, M. C. SWISS-MODEL and the Swiss-PdbViewer: An environment for comparative protein modelling. *Electrophoresis* **1997**, *18*, 2714−2723.

(20) Case, D. A.; Darden, T.; Cheatham, T. E., III; Simmerling, C. L.; Wang, J.; Duke, R. E.; Luo, R.; Merz, K. M.; Wang, B.; Pearlman, D. A.; Crowley, M.; Brozell, S.; Tsui, V.; Gohlke, H.; Mongan, J.; Hornak, V.; Cui, G.; Beroza, P.; Schafmeister, C.; Caldwell, J. W.; Ross, W. S.; Kollman, P. A. *Amber 8*; University of California: San Francisco, CA, 2004.

(21) Eriksson, M. A.; Roux, B. Modeling the structure of agitoxin in complex with the Shaker K^+ channel: a computational approach based on experimental distance restraints extracted from thermodynamic mutant cycles. *Biophys. J*. **2002**, *83*, 2595−2609.

(22) Cui, M.; Shen, J.; Briggs, J. M.; Fu, W.; Wu, J.; Zhang, Y.; Luo, X.; Chi, Z.; Ji, R.; Jiang, H.; Chen, K. Brownian dynamics simulations of the recognition of the scorpion toxin P05 with the small-conductance calcium-activated potassium channels. *J. Mol. Biol*. **2002**, *318*, 417−428.

(23) Tsui, V.; Case, D. A. Theory and application of the Generalized Born solvation model in macromolecular simulations. *Biopolymers* **2001**, *56*, 275−291.

(24) Wang, J.; Cieplak, P.; Kollman, P. A. How well does a RESP (Restrained Electrostatic Potential) Model do in calculating the conformational energies of organic and biological molecules? *J. Comput. Chem*. **2000**, *21*, 1049−1074.

(25) Yi, H.; Cao, Z. J.; Yin, S.; Dai, C.; Wu, Y. L.; Li, W. X. Interaction simulation of hERG K^+ channel with its specific Bekm-1 peptide: insights into the selectivity of molecular recognition. *J. Proteome Res.* **2007**, *6*, 611.

(26) Kalman, K.; Pennington, M. W.; Lanigan, M. D.; Nguyen, A.; Rauer, H.; Mahnir, V.; Paschetto, K.; Kem, W. R.; Grissmer, S.; Gutman, G. A.; Christian, E. P.; Cahalan, M. D.; Norton, R. S.; Chandy, K. G. ShK-Dap22, a potent Kv1.3-specific immunosuppressive polypeptide. *J. Biol. Chem*. **1998**, *273*, 32697−32707.

(27) Norton, R. S.; Pennington, M. W.; Wulff, H. Potassium channel blockade by the sea anemone toxin ShK for the treatment of multiple sclerosis and other autoimmune diseases. *Curr. Med. Chem*. **2004**, *11*, 3041−3052.

(28) Massova, I.; Kollman, P. A. Computational alanine scanning to probe protein−protein interactions: a novel approach to evalute binding free energies. *J. Am. Chem. Soc*. **1999**, *121*, 8133−8143.

(29) Mouhat, S.; Visan, V.; Ananthakrishnan, S.; Wulff, H.; Andreotti, N.; Grissmer, S.; Darbons, H.; De Waard, M.; Sabatier, J. M. K+ channel types targeted by synthetic OSK1, a toxin from *Orthochirus scrobiculosus* scorpion venom. *Biochem. J.* **2005**, *385*, 95−104.

(30) Mouhat, S.; Teodorescu, G.; Homerick, D.; Visan, V.; Wulff, H.; Wu, Y. L.; Grissmer, S.; Darbon, H.; De Waard, M.; Sabatier, J. M. Pharmacological profiling of *Orthochirus scrobiculosus* toxin 1 analogs with a trimmed N-terminal domain. *Mol. Pharmacol*. **2006**, *69*, 354−362.

(31) Kalman, K.; Pennington, M. W.; Lanigan, M. D.; Nguyen, A.; Rauer, H.; Mahnir, V.; Paschetto, K.; Kem, W. R.; Grissmer, S.; Gutman, G. A.; Christian, E. P.; Cahalan, M. D.; Norton, R. S.; Chandy, K. G. ShK-Dap,[22] a potent Kv1.3-specific immunosuppressive polypeptide. *J. Biol. Chem*. **1998**, *273*, 32697−32707.

(32) Lanigan, M. D.; Kalman, K.; Lefievre, Y.; Pennington, M. W.; Chandy, G.; Norton, R. S. Mutating a critical lysine in ShK toxin alters its binding configuration in the pore-vestibule region of the voltage-gated potassium channel, Kv1.3. *Biochemistry* **2002**, *41*, 11963−11971.

(33) Gilquin, B.; Braud, S.; Eriksson, M. A. L.; Roux, B.; Bailey, T. D.; Priest, B. T.; Garcia, M. L.; Menez, A.; Gasparini, S. A variable residue in the pore of Kv1 channels is critical for the high affinity of blockers from sea anemones and scorpions. *J. Biol. Chem*. **2005**, *280*, 27093−27102.

(34) Visan, V.; Fajloun, Z.; Sabatier, J. M.; Grissmer, S. Mapping of maurotoxin binding sites on hKv1.2, hKv1.3, and hIKCa1 channels. *Mol. Pharmacol*. **2004**, *66*, 1103−1112.

(35) Mouhat, S.; De Waard, M.; Sabatier, J. M. Contribution of the functional dyad of animal toxins acting on voltage-gated Kv1-type channels. *J. Pept. Sci*. **2004**, *11*, 65−68

(36) Lange, A.; Giller, K.; Hornig, S.; Martin-Eauclaire, M. F.; Pongs, O.; Becker, S.; Baldus, M. Toxin-induced conformational changes in a potassium channel revealed by solid-state NMR. *Nature* **2006**, *440*, 959−962.

CI700178W